Journal of Biomolecular NMR, 7 (1996) 283–294
ESCOM

J-Bio NMR 348

Backbone dynamics of an alamethicin in methanol and aqueous detergent solution determined by heteronuclear ^{1}H-^{15}N NMR spectroscopy

Leo Spyracopoulos, Adelinda A. Yee and Joe D.J. O'Neil*

Department of Chemistry, University of Manitoba, Winnipeg, MB, Canada R3T 2N2

Received 4 October 1995
Accepted 19 January 1996

Keywords: Alamethicin; Detergent; Backbone dynamics; Fungal peptide; ^{15}N NMR relaxation

Summary

The ^{15}N relaxation rates of the α-aminoisobutyric acid (Aib)-rich peptide alamethicin dissolved in methanol at 27 °C and 5 °C, and dissolved in aqueous sodium dodecylsulfate (SDS) at 27 °C, were measured using inverse-detected one- and two-dimensional ^{1}H-^{15}N NMR spectroscopy. Measurements of ^{15}N longitudinal ($R_N(N_z)$) and transverse ($R_N(N_{x,y})$) relaxation rates and the $\{^{1}H\}^{15}N$ nuclear Overhauser enhancement (NOE) at 11.7 Tesla were used to calculate (quasi-) spectral density values at 0, 50, and 450 MHz for the peptide in methanol and in SDS. Spectral density mapping at 0, 50, 450, 500, and 550 MHz was done using additional measurements of the ^{1}H-^{15}N longitudinal two-spin order, $R_{NH}(2H_z^N N_z)$, two-spin antiphase coherence, $R_{NH}(2H_z^N N_{x,y})$, and the proton longitudinal relaxation rate, $R_H(H_z^N)$, for the peptide dissolved in methanol only. The spectral density of motions was also modeled using the three-parameter Lipari–Szabo function. The overall rotational correlation times were determined to be 1.1, 2.5, and 5.7 ns for alamethicin in methanol at 27 °C and 5 °C, and in SDS at 27 °C, respectively. From the rotational correlation time determined in SDS the number of detergent molecules associated with the peptide was estimated to be about 40. The average order parameter was about 0.7 and the internal correlation times were about 70 ps for the majority of backbone amide ^{15}N sites of alamethicin in methanol and in SDS. The relaxation data, spectral densities, and order parameters suggest that the peptide N-H vectors of alamethicin are not as highly constrained as the 'core' regions of folded globular proteins. However, the peptide backbone is clearly not as mobile as the most unconstrained regions of folded proteins, such as those found in the 'frayed' C- and N-termini of some proteins, or in random-coil peptides. The data also suggest significant mobility at both ends of the peptide dissolved in methanol. In SDS the mobility in the middle and at the ends of the peptide is reduced. The implications of the results with respect to the sterically hindered Aib residues and the biological activities of the peptide are discussed.

Introduction

Understanding biological processes at the molecular level requires not only a knowledge of molecular structures at atomic resolution but a description of the changes in molecular conformation with time. NMR relaxation rate analysis is a powerful method for the investigation of motional processes in proteins on the millisecond to picosecond time scales (Wagner, 1993). Analysis of nuclear relaxation using model-independent formalism (Lipari and Szabo, 1982a,b) and spectral density mapping (Peng and Wagner, 1992a,b) has yielded a wealth of insight into the internal dynamics of proteins (Berglund et al., 1992; Redfield et al., 1992; Farrow et al., 1994; Shaw et al., 1995). In general, experiments have shown that NMR relaxation of backbone ^{13}C and ^{15}N atoms in folded globular proteins is dominated by overall molecular reorientation with a smaller component due to internal motion on a time scale shorter than that required for overall molecular diffusion (Wagner, 1993). Thus, the folding of long polypeptide chains into stable globular conformations restricts atomic motion in the backbone to low-amplitude diffusion (London, 1989). Many other interesting variations have also been observed attesting to the power of the methodology and the variety of motions that can occur in proteins. For example, intermediate and large amplitude motions have been detected in the loop regions of several proteins (Kördel et al., 1992; Redfield et al.,

*To whom correspondence should be addressed.

1992), in less structured regions of proteins (Peng and Wagner, 1992a,b), throughout the backbone of a folded protein (Powers et al., 1992), and in an unfolded protein (Farrow et al., 1995a). In addition, measurements of methine, methylene, and methyl ^{13}C relaxation measurements have revealed the dynamics of side-chain atoms in several proteins (Palmer et al., 1991; Nicholson et al., 1992; Kushlan and LeMaster, 1993).

Peptides consisting of fewer than 20 amino acids are usually flexible in solution and large-amplitude internal motions about single bonds prevent the formation of stable secondary or tertiary structures (Neuhaus and Williamson, 1989). Exceptions to this generalization include the many alanine-based peptides designed by Baldwin and co-workers (Scholtz et al., 1991), and others (Shalongo et al., 1994), and the α-aminoisobutyric acid (Aib)-based peptides found in the fungal antibiotics called peptaibols (Cafiso, 1994). The second α-methyl group in the Aib residue adds a steric restraint to motion about the ϕ and ψ angles which strongly constrains the residues to the right- or left-handed helical conformation (Burgess and Leach, 1973; Paterson et al., 1981; Toniolo et al., 1993). This observation has led to the suggestion that these residues might be useful in the design of stable helical segments in artificial proteins (Degrado and Lear, 1990; Karle and Balaram, 1990; Marshall et al., 1990). In the most well-studied peptaibol, alamethicin, dispersion of ^{1}H, ^{13}C, and ^{15}N chemical shifts suggests that the peptide, or at least parts of it, exist(s) in a stable helical conformation in methanol (Esposito et al., 1987; Yee et al., 1995) and in aqueous detergent solutions (Franklin et al., 1994). Homonuclear ^{1}H coupling constants and NOEs/ROEs also suggest that the peptide is partially helical. However, the lack of CH^{α} resonances at the eight Aib residues and the severe overlap of the α-methyls of the Aibs reduce the number of measurable NMR parameters (Esposito et al., 1987; Yee and O'Neil, 1992). This lack of data inevitably results in poorly constrained NMR solution structures and the temptation to interpret them as indicating a highly dynamic conformation in solution (Franklin et al., 1994; Yee et al., 1995).

Molecular dynamics/mechanics calculations have been used to investigate the apparent preference of Aib residues for the 3_{10} helix and the α-helix (Basu et al., 1994; Huston and Marshall, 1994) and to investigate the dynamics of alamethicin peptides on the femtosecond to picosecond time scales (Fraternalli, 1990). The dynamics of seven of the non-Aib α-carbons in alamethicin and some of the side chains were investigated by natural abundance ^{13}C NMR spectroscopy by Kelsh et al. (1992). Alamethicin is well-suited to relaxation-rate analysis, as it can be labelled with ^{15}N (Yee and O'Neil, 1992) and ^{13}C (Yee et al., 1996). To investigate the dynamics of alamethicin at both the L-amino acids and the Aib residues, we have measured residue-specific ^{15}N relaxation data for uniformly labelled alamethicin dissolved in methanol and in aqueous sodium dodecylsulfate (SDS) solution. The results have been analysed by the model-free approach of Lipari and Szabo (1982a,b), by the spectral density mapping method of Peng and Wagner (1992a,b), and by the quasi-spectral density mapping method (Farrow et al., 1995a,b; Ishima and Nagayama, 1995a,b).

Materials and Methods

Alamethicin was prepared and biosynthetically labelled with ^{15}N, as described previously (Yee and O'Neil, 1992). For this study two samples were prepared: in one, the peptide was dissolved in CD_3OH and diluted to about 1.5 mM, pH 7.4 and in the other it was diluted to about 1.6 mM in 20 mM sodium phosphate buffer, pH 5, 150 mM SDS, and 5% D_2O/95% H_2O.

NMR Spectroscopy

All one- and two-dimensional NMR spectra were acquired on a Bruker AMX 500 NMR spectrometer with a broadband 5-mm inverse probehead. The assignment of the proton resonances of alamethicin in SDS was done using the sequential assignment method (Wüthrich, 1986). Spin systems for the non-Aib residues were identified using HOHAHA (Bax and Davis, 1985) and DQF-COSY (Marion and Wüthrich, 1983). The ^{15}N resonances were assigned using the HMQC experiment (Bax et al., 1983) and HMQC-NOESY experiment (Shon and Opella, 1989). In the latter the mixing sequence following the HMQC portion of the pulse sequence allows for homonuclear ^{1}H magnetization exchange via cross-relaxation. Thus, the spectrum is a standard heteronuclear correlation map with intense ^{15}N-^{1}H cross peaks, but also contains weaker NOE cross peaks between sequential amide protons.

Conforming to the notation of Peng and Wagner (1992a), the following five relaxation rates for alamethicin in methanol at 5 °C and 27 °C were measured: $R_N(N_z)$, $R_N(N_{x,y})$, $R_{NH}(2H_z^N N_z)$, $R_{NH}(2H_z^N N_{x,y})$ and $R_H(H_z^N)$. The cross-relaxation rate $R_N(H_z^N \rightarrow N_z)$ was calculated from the $R_N(N_z)$ and the measured $\{^{1}H\}^{15}N$ NOE (Peng and Wagner, 1992a,b). The pulse sequences used for the measurement of $R_N(N_z)$ and $R_N(N_{x,y})$ were similar to those reported by Barbato et al. (1992), modified for one-dimensional acquisition (see Figs. 1a–c; Barbato et al., 1992). For the measurement of the $\{^{1}H\}^{15}N$ NOE, a pulse sequence similar to that shown in Fig. 1c from Kay et al. (1989) was used. The $R_{NH}(2H_z^N N_z)$, $R_{NH}(2H_z^N N_{x,y})$ and $R_H(H_z^N)$ were measured using the pulse sequences reported by Peng and Wagner, (see Figs. 2d–f; Peng and Wagner, 1992b). Suppression of the solvent signal was achieved by the use of high-power ^{1}H spin-lock pulses for all pulse sequences (Messerle et al., 1989). The refocusing delay for the INEPT transfers was set to $1/(4\,{}^{1}J_{NH})$ with ${}^{1}J_{NH} = 90$ Hz. The GARP sequence (Shaka et al., 1985) was used to decouple the ^{15}N spins during acquisition.

The one-dimensional data sets for the determination of the relaxation rates were obtained with 64 acquisitions, and consisted of 8K data points and a spectral width of 4762 Hz, with the ^{1}H carrier frequency centered on the solvent resonance. A relaxation delay of 4 s was used between scans. For the measurement of $R_N(N_z)$, nine experiments with delays of 25.1, 165.9, 316.7, 467.6, 618.5, 769.4, 920.2, 1071.1, and 1222.0 ms were used at 27 °C, and nine delays of 11.56, 152.44, 303.38, 454.31, 605.25, 756.19, 907.13, 1058.06, and 1209.00 ms were used in the experiments at 5 °C. Cross-correlation between dipolar and chemical shift anisotropy (CSA) relaxation was eliminated by applying ^{1}H 180° pulses every 5 ms during the parametrically varied relaxation delay (Boyd et al., 1990; Kay et al., 1992). The transverse relaxation rate $R_N(N_{x,y})$, was obtained via the CPMG technique and determined with nine delays of 7.5, 67.1, 126.8, 193.9, 253.5, 320.6, 380.3, 447.4, and 507.0 ms at 27 °C, and nine delays of 7.4, 67.0, 126.5, 193.4, 253.0, 320.0, 379.4, 446.4, and 505.9 ms at 5 °C. A delay of 0.9 ms was used between ^{15}N 180° pulses in the CPMG sequence. ^{1}H 180° pulses were applied every second echo to eliminate the effects of cross-correlation between dipolar and CSA relaxation (Goldman, 1984; Boyd et al., 1991; Kay et al., 1992; Palmer et al., 1992). The decay rate of longitudinal two-spin order, $R_{NH}(2H_z^N N_z)$, was determined from nine experiments having delays of 0.5, 80, 160, 240, 320, 400, 480, 560, and 640 ms at both 27 °C and 5 °C. For the measurement of the antiphase transverse relaxation rate, $R_{NH}(2H_z^N N_{x,y})$, a ^{15}N spin-lock field of 3 kHz centered at 96 ppm from external 2.9 M $^{15}NH_4Cl$ in 1 M HCl was used. The rate of decay was determined from nine experiments with delays of 8.2, 43.6, 87.2, 130.8, 174.4, 218.0, 261.7, 303.4, and 348.9 ms at 27 °C, and nine experiments with delays of 8.7, 49.4, 92.7, 139.1, 185.5, 231.8, 278.2, 322.5, and 370.9 ms at 5 °C. The longitudinal relaxation rates for the amide protons, $R_H(H_z^N)$, were determined from nine experiments with delays of 0, 100, 200, 300, 400, 500, 600, 700, and 800 ms at both 27 °C and 5 °C.

The heteronuclear NOE was obtained from two-dimensional spectra acquired with and without proton saturation. The solvent resonance was suppressed by the use of high-power ^{1}H-spin-lock pulses. The size of the data set was 512 points in the ^{1}H dimension (F2) and 64 points in the ^{15}N dimension (F1), with 72 scans acquired per t_1 increment for alamethicin dissolved in methanol at 27 °C. The data set was 1024 (F2) by 256 (F1) points, with 32 scans acquired per t_1 increment for alamethicin dissolved in methanol at 5 °C. The carrier was placed on the solvent resonance and the spectral width was 5051 Hz for ^{1}H. For ^{15}N, the carrier was set to 96 ppm from external 2.9 M $^{15}NH_4Cl$ in 1 M HCl and a spectral width of 2281 Hz was used. Quadrature detection was achieved by the use of TPPI (Marion and Wüthrich, 1983). For the data set acquired without the NOE, a delay of 6 s was used between scans. Proton saturation was achieved for the data set with NOE by applying ^{1}H 120° pulses every 20 ms for a total of 3.2 s.

The longitudinal and transverse relaxation rates, $R_N(N_z)$, $R_N(N_{x,y})$ respectively, and the heteronuclear $\{^1H\}^{15}N$ NOE of alamethicin dissolved in SDS were measured from two-dimensional spectra acquired at 27 °C. The pulse sequences were similar to those reported by Barbato et al. (1992). The data sets consisted of 1024 and 256 data points in F2 (^{1}H) and F1 (^{15}N), respectively. For the measurement of $R_N(N_z)$ and $R_N(N_{x,y})$, 32 scans per t_1 increment were acquired, with a delay between scans of 1.2 s. The NOE data sets were acquired with 64 scans per t_1 increment. The data set collected in the absence of proton saturation used a delay of 4 s between scans. The relaxation rates were obtained from eight experiments with delays of 27.0, 147.8, 273.6, 399.3, 525.1, 650.9, 776.6, and 902.4 ms for $R_N(N_z)$, and 7.5, 29.8, 52.1, 74.5, 96.8, 119.2, 141.5, and 163.9 ms for $R_N(N_{x,y})$. Other experimental details are as described for the experiments in methanol.

Spectra processing and analysis

The one-dimensional data sets were processed with 0.3-Hz line-broadening and an automatic baseline correction was applied. The relaxation rates were obtained by fitting peak heights obtained with the standard Bruker software to a two-parameter exponential decay as a function of relaxation delay. The two-dimensional data sets for the measurement of the heteronuclear NOE at 27 °C and 5 °C were zero-filled to 2K data points in F1 and 512 points in F2. The data sets were processed with a $\pi/2$-shifted sine-squared window function before Fourier transformation. Third and fifth order polynomial functions were subtracted from the baselines in F2 and F1, respectively. The values of the cross-peak integrals were obtained with the standard Bruker software.

Model-free spectral density analysis

When molecular motion occurs with a rate equal to that of one of the nuclear transition frequencies in the ^{15}N-^{1}H spin system, NMR relaxation may occur. The equations relating the macroscopic rates of relaxation and the heteronuclear NOE to the values of the spectral density at the nuclear spin transition frequencies $J(\omega)$ are given by Abragam (1961):

$$R_N(N_z) = D[J(\omega_H - \omega_N) + 3J(\omega_N) + 6J(\omega_H + \omega_N)] + CJ(\omega_N) \quad (1)$$

$$R_N(N_{x,y}) = \frac{D}{2}[4J(0) + J(\omega_H - \omega_N) + 3J(\omega_N) + 6J(\omega_H + \omega_N) + 6J(\omega_H)] + C\left[\frac{2}{3}J(0) + \frac{1}{2}J(\omega_N)\right] \quad (2)$$

$$NOE = 1+\eta = 1+\frac{\gamma_H}{\gamma_N}\left\{\frac{D[6J(\omega_H+\omega_N)-J(\omega_H-\omega_N)]}{R_N(N_z)}\right\} \quad (3)$$

where $D=(\mu_0/4\pi)^2(\gamma_H^2\gamma_N^2\hbar^2)/4r_{NH}^6$ and $C=(\Delta^2\omega_N^2)/3$. μ_0 is the permeability constant of free space ($4\pi\times10^{-7}$ kg m s^{-2} A^{-2}), γ_H is the proton gyromagnetic ratio (2.68×10^8 rad s^{-1} T^{-1}), γ_N is the gyromagnetic ratio of ^{15}N (-2.71×10^7 rad s^{-1} T^{-1}), r_{NH} is the proton–nitrogen internuclear separation (102 pm), Δ is the difference between the parallel and perpendicular components of the ^{15}N chemical shift tensor (−160 ppm), $\hbar$ is Planck's constant divided by 2π (1.05×10^{-34} J s), and $\omega_N=3.18\times10^8$ rad s^{-1}. Since an exact solution of Eqs. 1–3, which contain five unknowns, is impossible, Lipari and Szabo (1982a) derived a simplified spectral density $J(\omega)_{LS}$ by making the assumption that overall molecular reorientation and fast internal motions are independent:

$$J(\omega)_{LS} = \frac{2}{5}\left[\frac{S^2\tau_c}{1+(\omega\tau_c)^2}+\frac{(1-S^2)\tau}{1+(\omega\tau)^2}\right] \quad (4)$$

where $1/\tau=1/\tau_c+1/\tau_e$. The Lipari–Szabo 'model-free' spectral density reduces the number of unknown parameters in Eqs. 1–3 to three: S^2, the square of the generalized order parameter, which indicates the degree of spatial restriction of the internal motions of the N-H vectors, where a value of 1 corresponds to fully restricted N-Hs and a value of 0 indicates unrestricted motion (Lipari and Szabo, 1982a,b); τ_e, the effective internal correlation time, which is related to both the amplitude and the rate of internal motion; and τ_c, the overall correlation time for molecular reorientation.

For the determination of the model-free parameters S^2, τ_e, and τ_c two approaches were taken: in the first, the function in Eq. 5 was minimized over all residues by optimizing the values of S^2 and τ_e for each residue, whereas τ_c was a variable common to all residues:

$$f\{S_j^2,\tau_{e,j},\tau_c\} = \sum_{j=1}^{N}\sum_{i}\frac{\left(R_N(i)^j_{exp}-R_N(i)^j_{calc}\right)^2}{\left(\sigma^j_{R_N(i)_{exp}}\right)^2} + \frac{\left(NOE^j_{exp}-NOE^j_{calc}\right)^2}{\left(\sigma^j_{NOE_{exp}}\right)^2} \quad (5)$$

In Eq. 5: $i=N_z^H$, $N_{x,y}^H$; $j=1$ to N residues; the subscripts 'calc' and 'exp' refer to calculated and experimental data, respectively; $\sigma_{R_N(i)_{exp}}$ are the standard deviations of the fits of the relaxation data, and $\sigma_{NOE_{exp}}$ is the standard deviation of the NOE data, which was estimated from the rms noise in the baseplane of the 2D NOE spectra. In the second approach, the overall correlation time was held constant at the value determined from the minimization of the $R_N(N_z)/R_N(N_{x,y})$ relaxation ratio for the majority of residues (Kay et al., 1989; Palmer et al., 1991). The function in Eq. 5 was minimized for each residue separately (N minimizations) by optimizing the values of S^2 and τ_e. In separate analyses, a conformational exchange term (R_{ex}) was added to the contributions from dipole–dipole and CSA relaxation to account for the observed transverse relaxation. Function minimization was accomplished using the steepest descent function-minimization protocol within the program *Mathematica* (Wolfram, 1991). The errors in the optimized values of S^2 and τ_e were determined using Monte Carlo procedures (Palmer et al., 1991).

Quasi-spectral density mapping

The five spectral density values in Eqs. 1–3 can be reduced to three values by assuming that the high-frequency components, $J(\omega_H+\omega_N)$, $J(\omega_H)$, and $J(\omega_H-\omega_N)$ are equal and collectively make a small contribution to nuclear relaxation (Farrow et al., 1995a,b). This approach, termed quasi-spectral density (QSD) mapping (Ishima and Nagayama, 1995a,b), is valid for molecules with long molecular correlation times and in cases where internal motions make a negligible contribution to relaxation (Farrow et al., 1995a,b). QSD-mapping was used to analyze the relaxation data of alamethicin dissolved in methanol at 27 °C and 5 °C, and in SDS at 27 °C. The high-frequency spectral density values were replaced by a single spectral density component, $J^Q(\omega_h)$, in Eqs. 1–3. Analytical solutions to the new equations (Ishima and Nagayama, 1995; Eqs. 3–8) are given by Farrow et al. (1995b; Eqs. 5–7). The errors in the QSD values were determined by Monte Carlo analysis.

Spectral density mapping

For molecules with short τ_c the spectral density is expected to have significant power at high frequencies (Slichter, 1990). Measurements of the transverse and longitudinal two-spin relaxation rates and the relaxation rate of amide-proton longitudinal relaxation provide enough measurements for the extraction of the spectral density values at all nuclear spin transition frequencies (Peng and Wagner, 1992a, Eqs. 9–12). This method has the advantage that molecular motions can be characterized without making any assumptions about the separability of the time scales between the motions or about the contributions to relaxation from high-frequency motions. The values of the spectral densities, $J(0)$, $J(\omega_N)$, $J(\omega_H+\omega_N)$, $J(\omega_H)$, and $J(\omega_H-\omega_N)$ were calculated from the experimentally determined relaxation rates using Eqs. 13–17 from Peng and Wagner (1992a). The error analysis was carried out using a standard Monte Carlo analysis.

Results

Assignment of the ^1H and ^{15}N resonances in SDS

The ^1H NMR spectrum of alamethicin dissolved in SDS was assigned by Franklin et al. (1994). We indepen-

TABLE 1
^1H AND ^{15}N ASSIGNMENTS OF ^{15}N-LABELLED ALAMETHICIN DISSOLVED IN 150 mM SDS-d_{25}, 20 mM PHOSPHATE BUFFER AT pH 5 in 95%/5% H_2O/D_2O[a]

Residue	$^1H^N$ (ppm)	^{15}N (ppm)	Residue	$^1H^N$ (ppm)	^{15}N (ppm)
Aib[1]	8.47	139.16	Gly[11]	8.10	102.09
Pro[2]	–	na[b]	Leu[12]	8.22	120.25
Aib[3]	7.28	125.78	Aib[13]	8.32	133.41
Ala[4]	7.56	118.91	Pro[14]	–	na
Aib[5]	8.20	129.97	Val[15]	7.58	118.91
Ala[6]	8.06	116.22	Aib[16]	7.65	130.04
Gln[7]	7.82	116.37	Aib[17]	7.96	125.86
Aib[8]	7.94	130.04	Gln[18]	7.55	114.12
Val[9]	7.54	113.53	Gln[19]	7.81	117.56
Aib[10]	8.21	131.46	Phol[20]	7.08	121.30

[a] ^1H is referenced internally to DSS and ^{15}N is referenced to external 2.9 M $^{15}NH_4Cl$ in 1 M HCl, which resonates at 24.93 ppm relative to liquid NH_3.
[b] na = not assigned.

dently assigned the ^1H and ^{15}N resonances using ^{15}N-labelled peptide. Table 1 summarizes the ^{15}N assignments. Details of the assignment procedure and spectra can be found in supplementary material, available from the authors on request.

Relaxation measurements

Figure 1 shows examples of the decay curves for the $R_N(N_{x,y})$ measurements for alamethicin in methanol. The data were fit to single-exponential, two-parameter decay curves. The average errors of the $R_N(N_{x,y})$ fits were 1.5, 1.7, and 2.7% for alamethicin dissolved in methanol at 27 °C and 5 °C, and in SDS at 27 °C, respectively. For $R_N(N_z)$ the average errors of the fits were 2.0, 3.0, and 3.0%, for alamethicin in methanol at 27 °C and 5 °C, and in SDS at 27 °C, respectively. The errors of the fits of the other relaxation data acquired are given in the figure legends.

Figure 2 shows the backbone amide proton and nitrogen relaxation rates and heteronuclear $\{^1H\}^{15}N$ NOEs measured for alamethicin dissolved in methanol at 27 °C (dark grey bars) and 5 °C (light grey bars) and in SDS at 27 °C (black bars). The error bars in the figure indicate one standard deviation of the data from the fits and are very similar to the errors estimated from the Monte Carlo analysis of the results (see Methods). The average values and standard deviations of the relaxation parameters in methanol at 27 °C (and 5 °C) are as follows: $R_N(N_z)$, 1.63 ± 0.17 (1.98 ± 0.18) s^{-1}; $R_N(N_{x,y})$, 1.98 ± 0.22 (3.07 ± 0.36) s^{-1}; $R_{NH}(2H_z^N N_{x,y})$, 3.08 ± 0.19 (4.25 ± 0.36) s^{-1}; $R_{NH}(2H_z^N N_z)$, 2.83 ± 0.18 (3.68 ± 0.39) s^{-1}; $R_H(H_z^N)$, 1.76 ± 0.14 (1.66 ± 0.10) s^{-1}; $R_N(H_z^N \rightarrow N_z)$, 0.25 ± 0.02 (0.17 ± 0.02) s^{-1}. According to Peng and Wagner (1992a), the measured two-spin relaxation rates ($R_{NH}(2H_z^N N_z)$ and $R_{NH}(2H_z^N N_{x,y})$) will be approximately equal to the sums of the measured one-spin rates ($R_H(H_z^N)$ + $R_N(N_z)$ or $R_N(N_{x,y})$) and this is confirmed in the rates measured here. In comparison, the average $R_N(N_z)$ and $R_N(N_{x,y})$ rates are 2.4 s^{-1} and 5.0 s^{-1}, respectively in the 56-residue IgG-binding domain of streptococcal protein G (Barchi et al., 1994).

In general, the relaxation rates in methanol are faster at 5 °C than at 27 °C, indicative of longer rotational correlation times at the lower temperature. One exception is the rate of proton longitudinal relaxation ($R_H(H_z^N)$) at 5 °C, which is slightly slower than the rate at 27 °C (Fig. 2C). In addition, the heteronuclear cross-relaxation rates are faster at 27 °C than at 5 °C, but this is due to the larger (negative) NOE at the higher temperature. This NOE effect is expected at higher temperatures for more rapidly moving molecules. The $R_N(N_z)$ data at both temperatures (Fig. 2A) show a pronounced curvature as a function of amino acid sequence, rates of relaxation being generally slower at the ends of the molecule and increasing as the middle is approached. A similar pattern is observed, though less pronounced, in both sets of two-spin relaxation rates (Figs. 2D and 2E). Note however that experiments, in which presaturation of the water resonance between scans was used, show a reduced intensity for the Aib[1] resonance compared to experiments in which proton spin-lock pulses for water suppression were employed. This suggests that the data for Aib[1] may be affected by rapid hydrogen exchange at that residue. In spite of this, the data suggest enhanced motion on the ns to ps time scale at the ends of the molecule.

The averages of the $\{^1H\}^{15}N$ NOE values $(1+\eta)$ at 27 °C and 5 °C, are -0.5 ± 0.3 and 0.13 ± 0.19, respectively (see Fig. 2F). Like the $R_N(N_{x,y})$ data, the NOE data in methanol are more variable from residue to residue than the $R_N(N_z)$ data, although at both temperatures more neg-

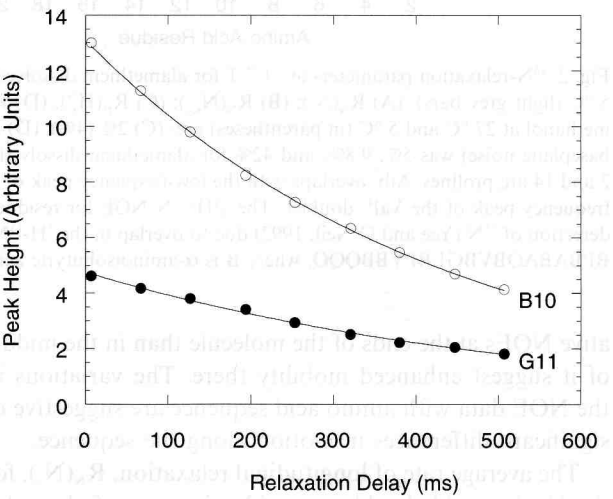

Fig. 1. Decay curves of transverse ($R_N(N_{x,y})$) ^{15}N magnetization for the best (open circles) and worst (filled circles) fits to a two-parameter single-exponential decay for alamethicin dissolved in methanol at 27 °C.

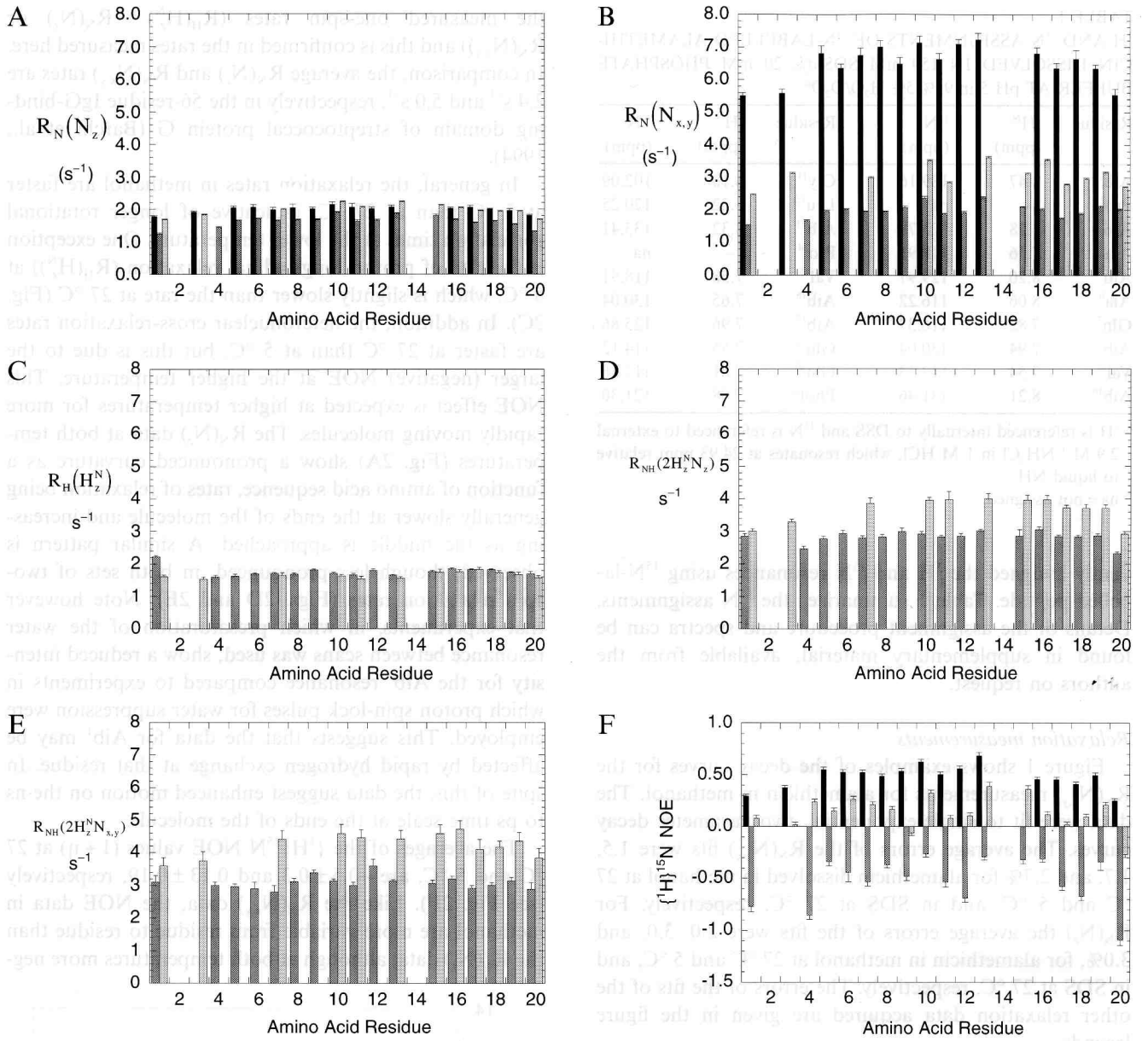

Fig. 2. ^{15}N-relaxation parameters at 11.7 T for alamethicin dissolved in SDS at 27 °C (black bars), and in methanol at 27 °C (dark grey bars) and 5 °C (light grey bars): (A) $R_N(N_z)$; (B) $R_N(N_{x,y})$; (C) $R_H(H_z^N)$; (D) $R_{NH}(2H_z^N N_z)$; (E) $R_{NH}(2H_z^N N_{x,y})$; and (F) $\{^1H\}^{15}N$ NOE. The average errors in methanol at 27 °C and 5 °C (in parentheses) are: (C) 2% (4%); (D) 3% (3%); (E) 4% (6%). The average error for the $\{^1H\}^{15}N$ NOE (from the rms baseplane noise) was 5%, 9.8%, and 42% for alamethicin dissolved in SDS at 27 °C, and in methanol at 27 °C and 5 °C, respectively. Residues 2 and 14 are prolines. Aib[3] overlaps with the low-frequency peak of the Val[15] doublet, thus measurements of $R_N(N_z)$ and $R_N(N_{x,y})$ are for the high-frequency peak of the Val[15] doublet. The $\{^1H\}^{15}N$ NOE for residues 6 and 19 of alamethicin in methanol at 27 °C (F) were measured by direct detection of ^{15}N (Yee and O'Neil, 1992) due to overlap in the ^1H-^{15}N 2D correlation spectrum. The amino acid sequence of alamethicin is: acetyl-BPBABAQBVBGLBPVBBQQO, where B is α-aminoisobutyric acid and O is phenylalaninol.

ative NOEs at the ends of the molecule than in the middle of it suggest enhanced mobility there. The variations in the NOE data with amino acid sequence are suggestive of significant differences in motion along the sequence.

The average rate of longitudinal relaxation, $R_N(N_z)$, for the 16 observable backbone amide nitrogens of alamethicin in SDS is 2.0 ± 0.1 s^{-1} and the transverse relaxation rate, $R_N(N_{x,y})$, has an average value of 6.5 ± 0.6 s^{-1} (see Figs. 2A,B; black bars). The average NOE $(1+\eta)$ is 0.5 ± 0.1 (see Fig. 2F; black bars). Compared to the relaxation rates measured in methanol, the $R_N(N_z)$ and especially the $R_N(N_{x,y})$ and NOE data are significantly less variable from residue to residue in SDS. The curvature in the data with respect to amino acid sequence is more pronounced for the $R_N(N_{x,y})$ and NOE data in SDS, suggesting greater mobility at the ends of the peptide. Excluding measurements at the end of the peptide, the longitudinal rates measured in SDS are slightly lower than those measured

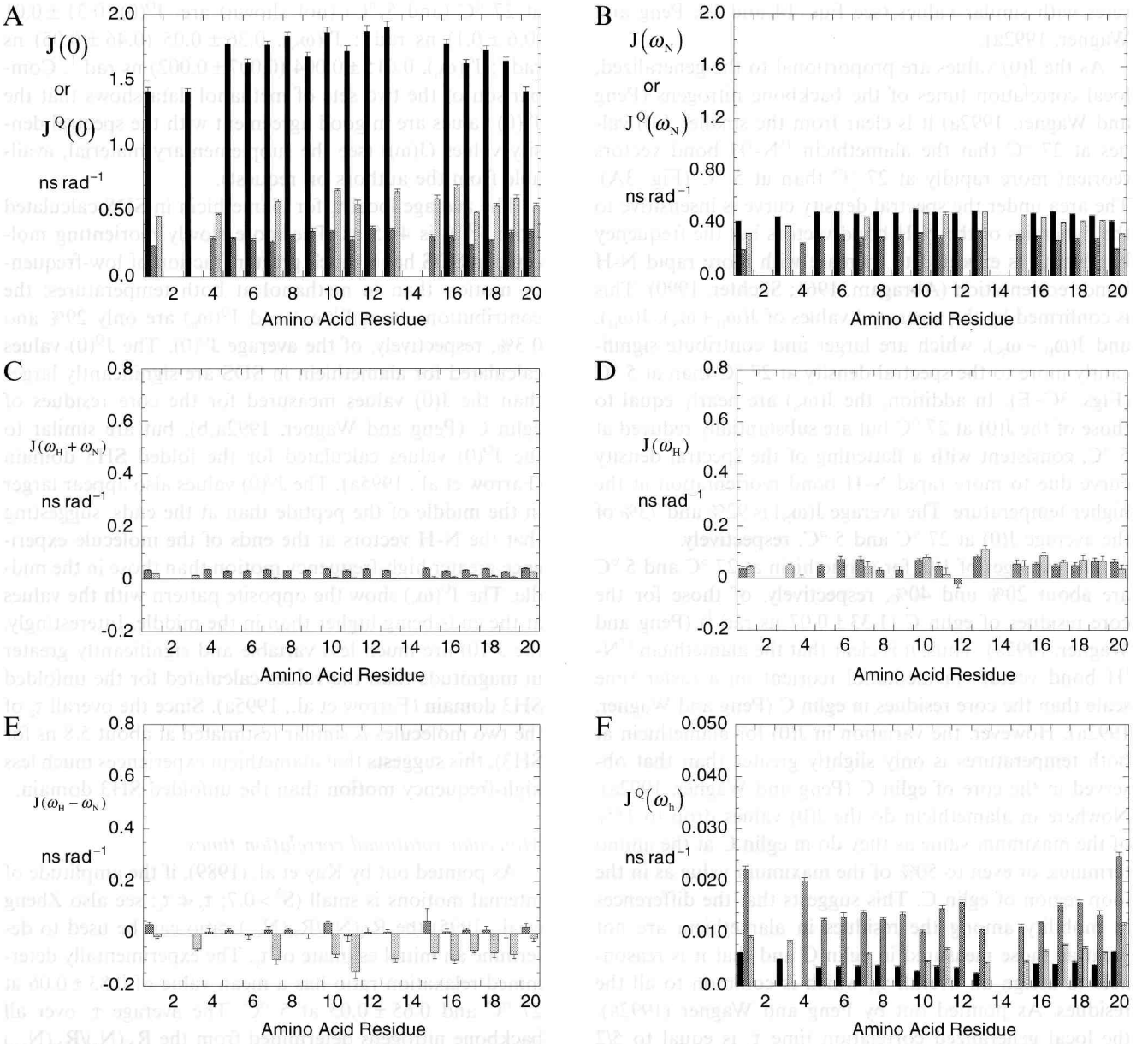

Fig. 3. ^{15}N spectral density values at 11.7 T of non-overlapped residues at 27 °C (dark grey bars) and 5 °C (light grey bars) for alamethicin in methanol: (A) J(0); (B) $J(\omega_N)$; (C) $J(\omega_H+\omega_N)$; (D) $J(\omega_H)$; (E) $J(\omega_H-\omega_N)$, in ns rad^{-1}. Errors are based on Monte Carlo analyses of the relaxation data (see Methods). Also shown are the quasi-spectral densities $J^Q(0)$ (A), and $J^Q(\omega_N)$ (B) for alamethicin dissolved in SDS at 27 °C (black bars), and $J^Q(\omega_h)$ (F) for the peptide in methanol at 27 °C (dark grey bars) and 5 °C (light grey bars), and in SDS (black bars) at 27 °C. Note the change of scale of the y-axis in Fig. 3F.

in methanol at 5 °C. This suggests that the addition of detergent has lengthened the overall τ_c to the extent that the peptide enters the spin-diffusion regime. In agreement with this, the $R_N(N_{x,y})$ rates are about twice as rapid in SDS at 27 °C compared to those measured in methanol at 5 °C. The measured NOEs are also significantly elevated in SDS compared to the values measured in methanol. However, the average NOE of 0.5 is significantly less than that predicted (0.75–0.8) for an isotropically rotating rigid molecule based on the measured $R_N(N_z)$ and $R_N(N_{x,y})$. This indicates that there are significant contributions to relaxation from high-frequency motion.

Spectral density mapping

Figure 3 shows the residue-specific values of the spectral density calculated at 0, ω_N, $\omega_H+\omega_N$, ω_H, and $\omega_H-\omega_N$ from the methanol relaxation data in Fig. 2 at 27 °C (dark grey bars) and 5 °C (light grey bars). The average values at 27 °C (and 5 °C) are: J(0), 0.30 ± 0.04 (0.57 ± 0.07) ns rad^{-1}; $J(\omega_N)$, 0.28 ± 0.04 (0.42 ± 0.06) ns rad^{-1}; $J(\omega_H+\omega_N)$, 0.034 ± 0.004 (0.010 ± 0.007) ns rad^{-1}; $J(\omega_H)$, 0.05 ± 0.03 (0.06 ± 0.03) ns rad^{-1}; and $J(\omega_H-\omega_N)$, 0.01 ± 0.02 (-0.07 ± 0.04) ns rad^{-1}. The negative values in the two sets of high-frequency data are likely due to the generation of the data by the subtraction of large relaxation

rates with similar values (see Eqs. 14 and 16; Peng and Wagner, 1992a).

As the J(0) values are proportional to the generalized, local correlation times of the backbone nitrogens (Peng and Wagner, 1992a) it is clear from the smaller J(0) values at 27 °C that the alamethicin ^{15}N-^{1}H bond vectors reorient more rapidly at 27 °C than at 5 °C (Fig. 3A). The area under the spectral density curve is insensitive to the dynamics of the N-H bond vectors but the frequency bandwidth is expected to increase with more rapid N-H bond reorientation (Abragam, 1961; Slichter, 1990). This is confirmed by the measured values of $J(\omega_H + \omega_N)$, $J(\omega_H)$, and $J(\omega_H - \omega_N)$, which are larger and contribute significantly more to the spectral density at 27 °C than at 5 °C (Figs. 3C–E). In addition, the $J(\omega_N)$ are nearly equal to those of the J(0) at 27 °C but are substantially reduced at 5 °C, consistent with a flattening of the spectral density curve due to more rapid N-H bond reorientation at the higher temperature. The average $J(\omega_N)$ is 92% and 73% of the average J(0) at 27 °C and 5 °C, respectively.

The averages of J(0) for alamethicin at 27 °C and 5 °C are about 20% and 40%, respectively, of those for the core residues of eglin C (1.33 ± 0.07 ns rad^{-1}) (Peng and Wagner, 1992a). Thus, it is clear that the alamethicin ^{15}N-^{1}H bond vectors in methanol reorient on a faster time scale than the core residues in eglin C (Peng and Wagner, 1992a). However, the variation in J(0) for alamethicin at both temperatures is only slightly greater than that observed in the core of eglin C (Peng and Wagner, 1992a). Nowhere in alamethicin do the J(0) values drop to 15% of the maximum value as they do in eglin C at the amino terminus, or even to 50% of the maximum value as in the loop region of eglin C. This suggests that the differences in mobility among the residues in alamethicin are not great as those measured in eglin C and that it is reasonable to assign an overall τ_c, which is common to all the residues. As pointed out by Peng and Wagner (1992a), the local generalized correlation time τ_c is equal to 5/2 J(0). The average J(0) value of 0.30 ± 0.04 ns rad^{-1} at 27 °C gives an average generalized correlation time of 0.8 ± 0.1 ns, and the average J(0) of 0.57 ± 0.07 ns rad^{-1} at 5 °C gives an average for the local correlation times of 1.4 ± 0.2 ns. The ratio of the averages for the local correlation times at 27 °C and 5 °C of 1.8 is in agreement with the theoretical ratio ($\tau_c^{5°}/\tau_c^{27°} = 1.8$) (see Discussion).

Calculation of three spectral density values $J^Q(0)$, $J^Q(\omega_N)$, and $J^Q(\omega_h)$ from two measured relaxation rates and the NOE allows comparison of the spectral density values measured in methanol with the QSD values calculated for alamethicin in SDS (see Fig. 3; panels A,B,F). The means and standard deviations of the quasi-spectral density values calculated for the molecule dissolved in SDS at 27 °C are: $J^Q(0)$, 1.6 ± 0.2 ns rad^{-1}; $J^Q(\omega_N)$, 0.47 ± 0.03 ns rad^{-1}; $J^Q(\omega_h)$, 0.004 ± 0.001 ns rad^{-1}. The means and standard deviations for the data in methanol at 27 °C (and 5 °C) (not shown) are: $J^Q(0)$, 0.31 ± 0.01 (0.6 ± 0.1) ns rad^{-1}; $J^Q(\omega_N)$, 0.36 ± 0.05 (0.46 ± 0.05) ns rad^{-1}; $J^Q(\omega_h)$, 0.015 ± 0.004 (0.007 ± 0.002) ns rad^{-1}. Comparison of the two sets of methanol data shows that the $J^Q(0)$ values are in good agreement with the spectral density values ($J(\omega)$) (see the supplementary material, available from the authors on request).

The average local τ_c for alamethicin in SDS calculated from $J^Q(0)$ is 4.25 ns. The more slowly reorienting molecule in SDS has a much greater fraction of low-frequency motion than in methanol at both temperatures; the contributions from $J^Q(\omega_N)$ and $J^Q(\omega_h)$ are only 29% and 0.3%, respectively, of the average $J^Q(0)$. The $J^Q(0)$ values calculated for alamethicin in SDS are significantly larger than the J(0) values measured for the core residues of eglin C (Peng and Wagner, 1992a,b), but are similar to the $J^Q(0)$ values calculated for the folded SH3 domain (Farrow et al., 1995a). The $J^Q(0)$ values also appear larger in the middle of the peptide than at the ends, suggesting that the N-H vectors at the ends of the molecule experience greater high-frequency motion than those in the middle. The $J^Q(\omega_h)$ show the opposite pattern with the values at the ends being higher than in the middle. Interestingly, the $J^Q(0)$ are much less variable and significantly greater in magnitude than the values calculated for the unfolded SH3 domain (Farrow et al., 1995a). Since the overall τ_c of the two molecules is similar (estimated at about 5.8 ns for SH3), this suggests that alamethicin experiences much less high-frequency motion than the unfolded SH3 domain.

Molecular rotational correlation times

As pointed out by Kay et al. (1989), if the amplitude of internal motions is small ($S^2 > 0.7$; $\tau_e \ll \tau_c$; see also Zheng et al., 1995) the $R_N(N_z)/R_N(N_{x,y})$ ratio can be used to determine an initial estimate of τ_c. The experimentally determined relaxation ratio has a mean value of 0.83 ± 0.06 at 27 °C and 0.65 ± 0.05 at 5 °C. The average τ_c over all backbone nitrogens determined from the $R_N(N_z)/R_N(N_{x,y})$ relaxation ratio is 1.2 ± 0.4 ns at 27 °C and 2.4 ± 0.3 ns at 5 °C. The τ_c at 27 °C is reduced to 1.1 ± 0.2 ns by excluding residues 17, 19, and 20, for which the τ_c values fall outside one standard deviation of the mean for all residues. The τ_c at 5 °C increases to 2.5 ± 0.3 ns by excluding residues 11 and 17, for which the overall correlation times are outside one standard deviation of the mean for all residues. The ratio of the calculated correlation times for alamethicin dissolved in methanol at 5 °C and 27 °C is $\tau_c^{5°}/\tau_c^{27°} = 1.8$ (assuming an isotropically reorienting sphere), compared to a ratio of 2.3 calculated from the correlation times obtained from the quotient $R_N(N_z)/R_N(N_{x,y})$.

The experimentally determined average $R_N(N_z)/R_N(N_{x,y})$ ratio determined for the molecule dissolved in SDS is 0.31 ± 0.02 for all residues. A correlation time for the overall molecular motion of 5.6 ± 0.2 ns was determined from the $R_N(N_z)/R_N(N_{x,y})$ ratio; this value was increased to 5.7 ± 0.1

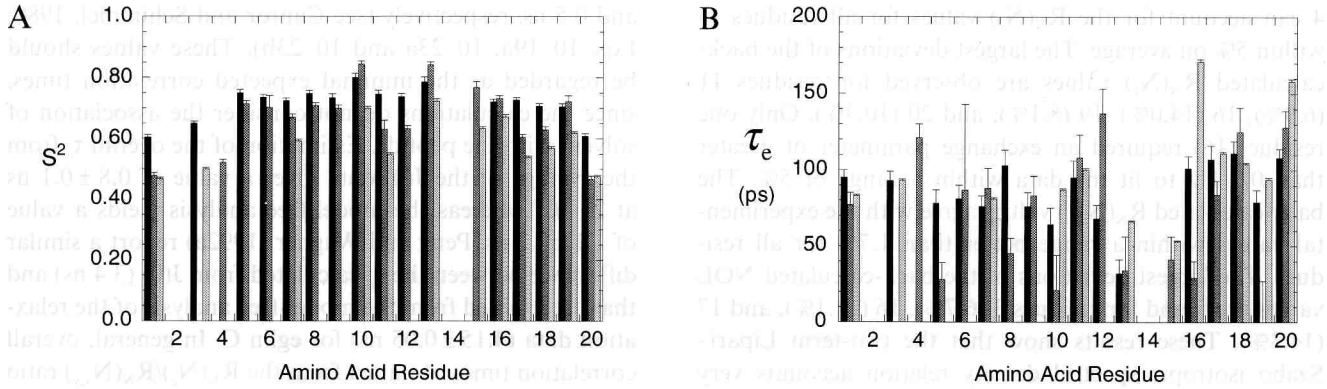

Fig. 4. (A) Order parameters (S^2) and (B) internal correlation times (τ_e) as a function of residue number for alamethicin dissolved in SDS at 27 °C (black bars), and in methanol at 27 °C (dark grey bars) and 5 °C (light grey bars). Errors are based on Monte Carlo analyses of the relaxation data.

ns by excluding the τ_c values for residues 3, 6, 12, 13, 17, and 20, for which the values are outside one standard deviation of the mean for all residues. This value is comparable to an average τ_c of 11 ns for the 50-residue bacteriophage-M13 coat protein dissolved in SDS at 23 °C, as measured by ^{13}C NMR relaxation studies of the methyl groups of [3-^{13}C]-labelled alanines (Henry et al., 1986).

Model-free analysis

The backbone dynamics of alamethicin dissolved in methanol were analyzed using the model-free approach of Lipari and Szabo (1982a,b), and a τ_c of 1.1 ns at 27 °C and 2.5 ns at 5 °C, as determined from the ratio $R_N(N_z)/R_N(N_{x,y})$. The model-free parameters S^2 and τ_e at 27 °C and 5 °C are shown in Fig. 4. The average order parameter at 27 °C is 0.7 ± 0.1, with a minimum value of 0.47 for residue 20 and a maximum value of 0.85 for residue 10. The average order parameter at 5 °C is 0.6 ± 0.1, with a maximum of 0.72 for residue 13 and a minimum of 0.47 for residue 1. At both temperatures the order parameters presented in Fig. 4 suggest that the motions of the N-H vectors at the ends of the molecule are less restricted than in the middle. Motions of the Gly[11] and Leu[12] NH bond vectors appear to be slightly greater than in the immediately adjacent residues.

The effective internal correlation times at 27 °C range from about 0 to 137 ps, with an average value of 73 ± 43 ps (see Fig. 4B). The average internal correlation time at 5 °C is 100 ± 34 ps, with a range of 53 to 158 ps. The internal correlation times, τ_e, depend on both the rate and amplitude of the internal motion, obfuscating a physical interpretation of their values outside a particular model for N-H bond motion (Lipari and Szabo, 1982a,b). A specific physical representation of the motion is Woessner's wobbling in a cone model (Woessner, 1962). Here, the cone semi-angle, θ_0, is related to the generalized order parameter through the relationship $(S^2)^{1/2} = 1/2(\cos\theta_0)(1+\cos\theta_0)$, which gives a cone semi-angle of 28° for an average order parameter of 0.7. The microscopic time constant for diffusion within this cone (τ_d) is calculated as 195 ps for Woessner's model, given an average internal correlation time of 73 ps (see Lipari and Szabo, 1982a, Eqs. A3 and A4; Kördel et al., 1992, Eqs. 7 and 8). In comparison to other globular proteins these parameters indicate moderately restricted internal motions of the N-H vectors in alamethicin at both temperatures.

Chemical shift, ROE, and circular dichroism measurements on alamethicin suggest that the molecule is less flexible at lower temperatures (Esposito et al., 1987; Yee et al., 1996). However, the measured order parameters do not seem to be sensitive to this difference (Fig. 4). It has been pointed out that the overall correlation time derived from the $R_N(N_z)/R_N(N_{x,y})$ ratio is not valid if $\tau_c < 1$ ns and $\tau_e > 100$ ps for backbone amide nitrogens in proteins (Kay et al., 1989). Thus, the overall correlation time and the internal motions must occur on different time scales. The data acquired for alamethicin at 27 °C are near this limit. However, the relaxation rates $R_N(N_z)$ and $R_N(N_{x,y})$, if back-calculated from the spectral density function and a τ_c of 1.1 ns for alamethicin at 27 °C, reproduce the experimental data for all residues to within 4%, except for residues 19 and 20. The back-calculated $R_N(N_z)$ rate for residue 20 is within 4% of the measured value and the $R_N(N_{x,y})$ rate within 22%. The calculated rates $R_N(N_z)$ and $R_N(N_{x,y})$ are within 6% and 8% of the experimental measurements for residue 19, respectively. The NOE data could be accurately reproduced within a range of 5% for all nitrogens, except for residues 11, 19, and 20 (ranges of 10%, 33% and 9%, respectively). The relaxation data for residues 19 and 20 could be accurately reproduced by including a conformational exchange term in the spectral density expression for $R_N(N_{x,y})$. When an exchange term is included, the optimized model-free parameters become: S^2 of 0.60 for residue 19, and 0.34 for residue 20; τ_e of 18 ps for residue 19 and 143 ps for residue 20; and exchange parameters of 0.3 Hz for residue 19 and 0.5 Hz for residue 20.

Relaxation rates were measured at 5 °C in order to move τ_c away from the $R_N(N_z) \approx R_N(N_{x,y})$ regime. The $R_N(N_z)/R_N(N_{x,y})$ ratio at 27 °C is 0.85, and this is reduced to 0.63 at 5 °C. The model-free parameters shown in Fig.

4 can account for the $R_N(N_z)$ values for all residues to within 5% on average. The largest deviations of the back-calculated $R_N(N_z)$ values are observed for residues 11 (6.9%), 16 (14.0%), 19 (8.1%), and 20 (10.3%). Only one residue (16) required an exchange parameter of greater than 0.3 Hz to fit the data within a range of 5%. The back-calculated $R_N(N_{x,y})$ values agree with the experimental values within a range better than 1.7% for all residues. The largest deviations of the back-calculated NOE values are found for residues 3 (6.7%), 16 (11.1%), and 17 (14.3%). These results show that the two-term Lipari–Szabo isotropic spectral density relation accounts very effectively for the relaxation data for alamethicin dissolved in methanol at 5 °C and at 27 °C .

Optimization of Eq. 5 on a per-residue basis with respect to S^2 and τ_e using the full Lipari–Szabo isotropic spectral density expression (see Eqs. 1–4) with an overall correlation time of 5.7 ns gives an average value for the order parameters of 0.72 ± 0.06 and a range of 0.61 to 0.81 for the peptide in SDS at 27 °C (see Fig. 4; black bars). The average effective internal correlation time is 92 ± 21 ps, with a maximum value of 126 ps and a minimum value of 36 ps. The order parameters and internal correlation times derived from the optimization account better than 99% for the experimental $R_N(N_{x,y})$ data and the $R_N(N_z)$ and NOE data better than 90% for all residues. The SDS relaxation data were also analyzed with a conformational exchange term as a free parameter in the spectral density expression for $R_N(N_{x,y})$ for all residues, except for residues 3, 6, and 17. The exchange terms vary from 0.1 Hz to 0.7 Hz with a mean value of 0.3 ± 0.2 Hz, indicating that conformational exchange on the μs- to ms-time scales makes only a minor contribution to $R_N(N_{x,y})$ for most residues.

As described in the Methods, we also analyzed the ^{15}N-relaxation data by minimizing Eq. 5 over all residues, optimizing the values of S^2 and τ_e for each residue, but taking τ_c as a variable common to all residues. The τ_c values estimated by this analysis were 1.1 ns for methanol at 27 °C, 2.7 ns for methanol at 5 °C, and 5.9 ns for SDS at 27 °C, in close agreement with the values estimated from the $R_N(N_z)/R_N(N_{x,y})$ ratio. Furthermore, the optimized values of S^2 and τ_e obtained from the latter analysis agree very well with the results of the former analysis.

Discussion

Rotational correlation times

Assuming a spherical shape for alamethicin in methanol, the molecular correlation time can be calculated from first principles, which yields a value of 0.3 ns at 30 °C (see Creighton, 1993; Eq. 7.6). If we assume that alamethicin is a prolate ellipsoid with a length of 30 Å (Fox and Richards, 1982), the correlation times for rotation about the long and short axes are calculated to be 0.2 and 0.5 ns, respectively (see Cantor and Schimmel, 1980; Eqs. 10–19a, 10–23a and 10–23b). These values should be regarded as the minimal expected correlation times, since the calculations do not consider the association of solvent with the peptide. Estimation of the overall τ_c from the average of the J(0) data gives a value of 0.8 ± 0.1 ns at 27 °C, whereas the model-free analysis yields a value of 1.1 ± 0.2 ns. Peng and Wagner (1992a) report a similar difference between the τ_c calculated from J(0) (3.4 ns) and that determined from the model-free analysis of the relaxation data (4.15 ± 0.05 ns) for eglin C. In general, overall correlation times obtained from the $R_N(N_z)/R_N(N_{x,y})$ ratio are, to a first approximation, independent of small-amplitude fast internal motions. By contrast, the local correlation times obtained from J(0) are weighted averages of overall and fast internal correlation times, and thus are expected to be slightly shorter than the τ_c obtained from the $R_N(N_z)/R_N(N_{x,y})$ ratio. The estimate of τ_c for alamethicin from the model-free analysis is in good agreement with the published values observed for similar molecules. For example, the τ_c determined for the cyclic 11-residue peptide cyclosporin A dissolved in $CDCl_3$ at 25 °C, based on ^{13}C relaxation measurements is 0.475 ns (Dellwo and Wand, 1989). The value of 1.88 ns for the 25-residue globular zinc-finger DNA-binding domain Xfin-31 dissolved in H_2O at 30 °C as determined by ^{13}C-NMR-relaxation measurements (Palmer et al., 1991), is also comparable to the correlation time for alamethicin dissolved in methanol at 27 °C.

Determination of the rotational correlation time of the alamethicin–detergent complex can be used to estimate the size of the complex. The τ_c value of 5.7 ± 0.1 ns for the peptide–detergent complex dissolved at 27 °C obtained from the model-free analysis can be used to calculate the mass of the complex, assuming it is spherical. From the known masses of the peptide and detergent monomers the number of detergent molecules in the complex is estimated to be about 40. It has been estimated by Henry et al. (1986) that approximately 60 SDS monomers are bound per M13 coat protein, however this protein has a sizable polar region that may not interact with the detergent in the same fashion as a highly hydrophobic peptide.

Anisotropic analysis

For seven of the 20 backbone α-carbons in alamethicin dissolved in methanol at 25 °C the dynamics have been reported by Kelsh et al. (1992), as determined by measurements of ^{13}C $R_C(C_z)$ and heteronuclear NOEs at 125 and 75 MHz. Their carbon relaxation data were fit to both an isotropic spectral density as well as to an anisotropic one, which is applicable if the molecule is a rigid helix. In an axially symmetric rigid helix the N-H bond vectors are aligned nearly parallel to the long axis of the helix. Rotation of the helix about its axis will not change the orientation of the N-H bond vectors relative to the

applied magnetic field (Barbato et al., 1992). Therefore the only motion that can give rise to ^{15}N relaxation is reorientation of the helix axis. The result is that the anisotropic ^{15}N spectral density reduces to the isotropic form for a rigid helix (Woessner, 1962; Huntress, 1968; Hubbard, 1970; Barbato et al., 1992, Eqs. 3–6). The analysis of ^{15}N relaxation rates of a rigid helix using an isotropic spectral density should give rise to order parameters near one and rapid (< 10 ps) internal motions. The excellent fits of the ^{15}N relaxation data to the Lipari–Szabo spectral density show that the dynamics of alamethicin are effectively described by an isotropic reorientation on the ns time scale with internal motions on the 10–100-ps time scale. The S^2 values near 0.7 suggest that 30% of the relaxation is due to fast internal motions with a significant Woessner wobbling angle of about 30°, contrary to the predictions for a rigid anisotropic helical model.

The ^{15}N relaxation data for alamethicin, analyzed both by the model-free and spectral density mapping techniques, suggest that generally the peptide N-H vectors are not as highly constrained as the 'core' regions of folded globular proteins. However, the peptide backbone is clearly not as mobile as the most unconstrained regions of folded proteins such as in the 'frayed' C- and N-termini of some proteins, which show order parameters as low as 0.2 (Stone et al., 1992; Barbato et al., 1992; Peng and Wagner, 1992a,b). Alamethicin is also more constrained than 42% of the residues in the unfolded SH3 domain with order parameters of less than 0.35, and than 83% of the residues with order parameters of less than 0.57 (Farrow et al., 1995a). Recently, model-free analysis of the relaxation data of 10-residue 'random-coil' peptides showed that these molecules have an average order parameter of 0.36 (Jarvis and Craik, 1995). The order parameters in alamethicin, with average values of about 0.7, suggest that this peptide is significantly more structured than the random-coil peptides. The restricted mobility of the alamethicin peptide is likely due to the steric constraints at the eight Aib residues and the cooperative energy effects associated with them (Aleman, 1994).

On average, the order parameters measured in SDS are greater by only 0.05 compared to those measured in methanol at 27 °C, suggesting little difference in dynamics between the two states of the peptide. The order parameters and spectral densities suggest that the ends of the peptide are more constrained in SDS than in methanol and that the peptide is less flexible near Gly^{11} in SDS. Thus, association with a detergent appears to damp out some of the variations in motion along the peptide observed in methanol. This is likely due to weakened interactions with water caused by the presence of the detergent, which thereby increases the stability of intramolecular hydrogen bonds. The chemical shifts of the $^{13}C^{\alpha}$ resonances confirm this interpretation (unpublished observation by A. Yee and J. O'Neil). This result is also in accord with CD data which indicate that the peptide dissolved in methanol is about 35% helical at 25 °C (Yee et al., 1996), and about 80% helical when dissolved in SDS at 25 °C (unpublished observations by A. Yee and J. O'Neil). CD spectra exhibiting less than 100% helicity are strongly suggestive of dynamic averaging of the helical conformation, which appears to be greater in methanol than in SDS.

Biological implications of the dynamics

Whereas the helical propensity of Aib residues is usually explained by the steric hindrance introduced by the substitution of the α-CH by an α-methyl, it is clear from the dynamics measurements presented here that there are not large differences between the dynamics of the Aib residues and the L-amino acids, even including glycine. For example, in all cases the order parameters measured for Aib^3 are always less than those measured for Gly^{11}. The average Aib order parameters (excluding Aib^1) are 0.75, 0.63 , and 0.74 in methanol at 27 °C and 5 °C, and in SDS at 27 °C, respectively. The average L-amino acid order parameters (excluding Gly^{11} and $Phol^{20}$) are 0.67, 0.60, and 0.72 in methanol at 27 °C and 5 °C, and in SDS at 27 °C, respectively.

Several models have been postulated to account for the voltage-gated ion-channel activity of alamethicin (see Sansom, 1993, and references therein). The relaxation data presented here are in accord with a model in which a peptide helix interacts with an applied voltage via its macrodipole. A highly dynamic peptide might be expected to have a significantly weaker helical macrodipole and thus would respond less readily to an applied voltage. On the other hand, the dynamic data do not rule out a model in which voltage regulation is mediated by a conformational change such as an $\alpha \rightarrow 3_{10}$ switch (Huston and Marshall, 1994).

As the fungus *Trichoderma viride* secretes alamethicin into its environment as a defense mechanism, its solubility in both polar and nonpolar media may be important to its usefulness as an antibiotic. In studies of a synthetic analog of alamethicin in which all the Aib residues are replaced by alanines, we have observed that the analog is significantly less helical and less soluble than alamethicin in several polar and nonpolar media (unpublished observations by J. O'Neil). The present results show that the alamethicin helix is much more stable on the ns–ps time scale than would be expected for such a small peptide. Maintaining the peptide poised in a stable helical conformation may be important to its antibiotic activity and may help to keep it soluble in solvents of different polarity.

Acknowledgements

The financial assistance of the Natural Sciences and

Engineering Research Council and the University of Manitoba is gratefully acknowledged. We thank Mr. Kirk Marat and Mr. Terry Wolowiec for maintenance of the NMR spectrometers.

References

Abragam, A. (1961) *Principles of Nuclear Magnetism*, Clarendon Press, Oxford, U.K.

Aleman, C. (1994) *Biopolymers*, **34**, 841–847.

Barbato, G., Ikura, M., Kay, L.E., Pastor, R.W. and Bax, A. (1992) *Biochemistry*, **31**, 5269–5278.

Barchi Jr., J.J., Grasberger, B., Gronenborn, A. and Clore, G.M. (1994) *Protein Sci.*, **3**, 15–21.

Basu, G., Kitao, A., Hirata, F. and Go, N. (1994) *J. Am. Chem. Soc.*, **116**, 6307–6315.

Bax, A., Griffey, R.H. and Hawkins, B.L. (1983) *J. Magn. Reson.*, **55**, 301–315.

Bax, A. and Davis, D.G. (1985) *J. Magn. Reson.*, **65**, 355–360.

Berglund, H., Kovács, H., Dahlman-Wright, K., Gustafsson, J. and Härd, T. (1992) *Biochemistry*, **31**, 12001–12001.

Boyd, J., Hommel, U. and Campbell, I.D. (1990) *Chem. Phys. Lett.*, **175**, 477–482.

Boyd, J., Hommel, U. and Krishnan, V.V. (1991) *Chem. Phys. Lett.*, **187**, 317–324.

Burgess, A.W. and Leach, S.J. (1973) *Biopolymers*, **12**, 2599–2605.

Cafiso, D.S. (1994) *Annu. Rev. Biophys. Biomol. Struct.*, **23**, 141–165.

Cantor, C.R. and Schimmel, P.R. (1980) *Biophysical Chemistry, Part II: Techniques for the Study of Biological Structure and Function*, Freeman, New York, NY, pp. 561–563.

Creighton, T.E. (1993) *Proteins: Structure and Molecular Properties*, Freeman, New York, NY, p. 268.

Dellwo, M.J. and Wand, A.J. (1989) *J. Am. Chem. Soc.*, **11**, 4571–4578.

Degrado, W.F. and Lear, J.D. (1990) *Biopolymers*, **27**, 205–213.

Esposito, G., Carver, J.A., Boyd, J. and Campbell, I.D. (1987) *Biochemistry*, **26**, 1043–1050.

Farrow, N.A., Munhandiram, R., Singer, A.U., Pascal, S.M., Kay, C.M., Gish, G., Shoelson, S.E., Pawson, T., Forman-Kay, J.D. and Kay, L.E. (1994) *Biochemistry*, **33**, 5984–6003.

Farrow, N.A., Zhang, O., Forman-Kay, J.D. and Kay, L.E. (1995a) *Biochemistry*, **34**, 868–878.

Farrow, N.A., Zhang, O., Szabo, A., Torchia, D.A. and Kay, L.E. (1995b) *J. Biomol. NMR*, **6**, 153–162.

Fox, R.O. and Richards, F.M. (1982) *Nature*, **300**, 325–330.

Franklin, J.C., Ellena, J.F., Jayasinghe, S., Kelsh, L.P. and Cafiso, D.S. (1994) *Biochemistry*, **33**, 4036–4045.

Fraternalli, F. (1990) *Biopolymers*, **30**, 1083–1099.

Goldman, M. (1984) *J. Magn. Reson.*, **60**, 437–452.

Henry, G.D., Weiner, J.H. and Sykes, B.D. (1986) *Biochemistry*, **25**, 590–598.

Hubbard, P.S. (1970) *J. Chem. Phys.*, **52**, 563–568.

Huntress, W.T. (1968) *J. Chem. Phys.*, **48**, 3524–3533.

Huston, S.E. and Marshall, G.R. (1994) *Biopolymers*, **34**, 75–90.

Ishima, R. and Nagayama, K. (1995a) *Biochemistry*, **34**, 3162–3171.

Ishima, R. and Nagayama, K. (1995b) *J. Magn. Reson. Ser. B*, **108**, 73–76.

Jarvis, J. and Craik, D.J. (1995) *J. Magn. Reson. Ser. B*, **107**, 95–106.

Karle, I. and Balaram, P. (1990) *Biochemistry*, **29**, 6747–6761.

Kay, L.E., Torchia, D.A. and Bax, A. (1989) *Biochemistry*, **28**, 8972–8979.

Kay, L.E., Nicholson, L.K., Delaglio, F., Bax, A. and Torchia, D.A. (1992) *J. Magn. Reson.*, **97**, 359–375.

Kelsh, L.P., Ellena, J.F. and Cafiso, D.S. (1992) *Biochemistry*, **31**, 5136–5144.

Kördel, J., Skelton, N.J., Akke, M., Palmer III, A.G. and Chazin, W.J. (1992) *Biochemistry*, **31**, 4856–4866.

Kushlan, D.M. and LeMaster, D.M. (1993) *J. Am. Chem. Soc.*, **115**, 11026–11027.

Lipari, G. and Szabo, A. (1982a) *J. Am. Chem. Soc.*, **104**, 4546–4559.

Lipari, G. and Szabo, A. (1982b) *J. Am. Chem. Soc.*, **104**, 4559–4570.

London, R.E. (1989) *Methods Enzymol.*, **176**, 358–375.

Marion, D. and Wüthrich, K. (1983) *Biochem. Biophys. Res. Commun.*, **113**, 967–974.

Marshall, G.R., Hodgkin, E.E., Langs, D.A., Smith, G.D., Zabrocki, J. and Leplawy, M.T. (1990) *Proc. Natl. Acad. Sci. USA*, **87**, 487–491.

Messerle, B.A., Wider, G., Otting, G., Weber, C. and Wüthrich, K. (1989) *J. Magn. Reson.*, **85**, 608–613.

Neuhaus, D. and Williamson, M.P. (1989) *The Nuclear Overhauser Effect in Structural and Conformational Analysis*, p. 463, VCH Publishers, New York, NY.

Nicholson, L.K., Kay, L.E., Baldisseri, D.M., Arango, J., Young, P.E., Bax, A. and Torchia, D.A. (1992) *Biochemistry*, **31**, 5253–5263.

Palmer III, A.G., Rance, M. and Wright, P.E. (1991) *J. Am. Chem. Soc.*, **113**, 4371–4380.

Palmer III, A.G., Skelton, N.J., Chazin, W.J., Wright, P.E. and Rance, M. (1992) *Mol. Phys.*, **75**, 699–711.

Paterson, Y., Rumsey, S.M., Benedetti, E., Nemethy, G. and Scheraga, H.A. (1981) *J. Am. Chem. Soc.*, **103**, 2947–2955.

Peng, J.W. and Wagner, G. (1992a) *Biochemistry*, **31**, 8571–8586.

Peng, J.W. and Wagner, G. (1992b) *J. Magn. Reson.*, **98**, 308–332.

Powers, R., Clore, G.M., Stahl, S.J., Wingfield, P.T. and Gronenborn, A. (1992) *Biochemistry*, **31**, 9150–9157.

Redfield, C., Boyd, J., Smith, L.J., Smith, A., G. and Dobson, C.M. (1992) *Biochemistry*, **31**, 10431–10437.

Sansom, M.S.P. (1993) *Eur. Biophys. J.*, **22**, 105–124.

Scholtz, J.M., Qian, H., York, E.J., Stewart, J.M. and Baldwin, R.L. (1991) *Biopolymers*, **31**, 1463–1470.

Shaka, A.J., Barker, P.B. and Freeman, R. (1985) *J. Magn. Reson.*, **64**, 547–552.

Shalongo, W., Dugald, L. and Stellewagen, E. (1994) *J. Am. Chem. Soc.*, **116**, 2500–2507.

Shaw, G.L., Davis, B., Keeler, J. and Fersht, A.R. (1995) *Biochemistry*, **34**, 2225–2233.

Shon, K. and Opella, S.J. (1989) *J. Magn. Reson.*, **82**, 193–197.

Slichter, C.P. (1990) *Principles of Magnetic Resonance*, 3rd ed., Springer-Verlag, Berlin, Germany.

Stone, M.J., Fairbrother, W.J., Palmer III, A.G., Reizer, J., Saier Jr., M.H. and Wright, P.E. (1992) *Biochemistry*, **31**, 4394–4406.

Toniolo, C., Crisma, M., Formaggio, F., Valle, G., Cavicchiono, G., Precigoux, G., Aulory, A. and Kauphais, J. (1993) *Biopolymers*, **33**, 1061–1072.

Wagner, G. (1993) *Curr. Opin. Struct. Biol.*, **3**, 748–754.

Woessner, D.T. (1962) *J. Chem. Phys.*, **37**, 647–654.

Wolfram, S. (1991) *Mathematica: A System for Doing Mathematics by Computer*, Addison-Wesley, New York, NY, pp. 703–704.

Wüthrich, K. (1986) *NMR of Proteins and Nucleic Acids*, Wiley, New York, NY.

Yee, A.A. and O'Neil, J.D.J. (1992) *Biochemistry*, **31**, 3135–3143.

Yee, A.A., Babiuk, R.P. and O'Neil, J.D.J. (1995) *Biopolymers*, **36**, 781–797.

Yee, A.A., Marat, K. and O'Neil, J.D.J. (1996) submitted for publication.

Zheng, Z., Czaplicki, J. and Jardetzky, O. (1995) *Biochemistry*, **34**, 5212–5223.